J Physiol 587.3 (2009) pp 567–586

The Journal of Physiology

Strain-specific genetics, anatomy and function of enteric neural serotonergic pathways in inbred mice

Kathleen B. Neal[1], Laura J. Parry[2] and Joel C. Bornstein[1]

[1] *Departments of Physiology and* [2] *Zoology, The University of Melbourne, Parkville, VIC, Australia*

Serotonin (5-HT) powerfully affects small intestinal motility and 5-HT-immunoreactive (IR) neurones are highly conserved between species. 5-HT synthesis in central neurones and gastrointestinal mucosa depends on tissue-specific isoforms of the enzyme tryptophan hydroxylase (TPH). RT-PCR identified strain-specific expression of a polymorphism (1473C/G) of the *tph2* gene in longitudinal muscle–myenteric plexus preparations of C57Bl/6 and Balb/c mice. The former expressed the high-activity C allele, the latter the low-activity G allele. Confocal microscopy was used to examine close contacts between 5-HT-IR varicosities and myenteric neurones immunoreactive for neuronal nitric oxide synthase (NOS) or calretinin in these two strains. Significantly more close contacts were identified to NOS- ($P < 0.05$) and calretinin-IR ($P < 0.01$) neurones in C57Bl/6 jejunum (NOS 1.6 ± 0.3, $n = 52$; calretinin 5.2 ± 0.4, $n = 54$), than Balb/c jejunum (NOS 0.9 ± 0.2, $n = 78$; calretinin 3.5 ± 0.3, $n = 98$). Propagating contractile complexes (PCCs) were identified in the isolated jejunum by constructing spatiotemporal maps from video recordings of cannulated segments *in vitro*. These clusters of contractions usually arose towards the anal end and propagated orally. Regular PCCs were initiated at intraluminal pressures of 6 cmH_2O, and abolished by tetrodotoxin (1 μM). Jejunal PCCs from C57Bl/6 mice were suppressed by a combination of granisetron (1 μM, 5-HT_3 antagonist) and SB207266 (10 nM, 5-HT_4 antagonist), but PCCs from Balb/c mice were unaffected. There were, however, no strain-specific differences in sensitivity of longitudinal muscle contractions to exogenous 5-HT or blockade of 5-HT_3 and 5-HT_4 receptors. These data associate a genetic difference with significant structural and functional consequences for enteric neural serotonergic pathways in the jejunum.

(Received 30 July 2008; accepted after revision 1 December 2008; first published online 8 December 2008)

Corresponding author K. B. Neal: Department of Physiology, The University of Melbourne, Parkville, VIC, Australia. Email: kbneal@unimelb.edu.au

Serotonin (5-HT) powerfully affects the motility of the GI tract *in vivo* and *in vitro* (for reviews see: Gershon, 2004; Neal & Bornstein, 2006; Galligan & Parkman, 2007). Behaviour characterized by regular, propagating complexes of contractions is modulated by 5-HT acting primarily through 5-HT_3 receptors in isolated mouse small intestine and colon (Fida *et al.* 2000; Bush *et al.* 2001). Such behaviour observed *in vitro* has been described as peristalsis or migrating motor complexes (MMCs), but may not be equivalent to either *in vivo* phenomenon; for example, its relationship to the fluid dynamics of luminal content is unknown. The term 'propagating contractile complexes' (PCCs) is preferred here, to avoid prejudging the functional relationship between *in vitro* and *in vivo* phenomena. Evidence also suggests that 5-HT_4 receptors may also be involved in control of propulsive activity in the small (Nagakura *et al.* 1997) and large (Kadowaki *et al.* 1996; Yamamoto *et al.* 1999) intestine *in vivo*. Enteric neurones that label for 5-HT are highly conserved between species (Costa *et al.* 1982; Barbiers *et al.* 1995; Sang *et al.* 1997; Anlauf *et al.* 2003), suggesting their role is fundamental. However, since 5-HT has been implicated both in transduction of sensory stimuli from the mucosa to sensory neurones and in neurotransmission within the enteric nervous system (ENS; Grider *et al.* 1996, 1998; Tonini, 2005; Galligan & Parkman, 2007; Gershon & Tack, 2007), the relative contribution of 5-HT from mucosal or neural sources to complex motility patterns is yet to be demonstrated conclusively.

5-HT synthesis is a two-step process in which tryptophan hydroxylase (TPH) is the first and rate-limiting step (Walther & Bader, 2003). Synthesis persists in classical serotonergic brain regions after knockout of the original *tph* gene in mice, hence a second

DOI: 10.1113/jphysiol.2008.160416

TPH isoform is responsible for 5-HT production in the central nervous system (CNS; Côté *et al.* 2003; Walther *et al.* 2003). This second TPH isoform, known as TPH2, is encoded by a unique gene, *tph2* (Côté *et al.* 2003; Walther *et al.* 2003). Indirect evidence that *tph2* is expressed in enteric neurones has been presented (Côté *et al.* 2003; Walther *et al.* 2003), and a preliminary study reported *tph2* mRNA expression in enteric neurones and their progenitors (Chen *et al.* 2004), but this remains to be conclusively demonstrated.

A polymorphism in murine *tph2* at nucleotide position 1473 has been described that profoundly affects the activity of the TPH2 enzyme and consequent levels of 5-HT in brain (Zhang *et al.* 2004). The 1473C allele encodes a proline (CCC) at residue 447, while the 1473G allele encodes arginine (CGC), with significant effects on the kinetic parameters of the enzyme; TPH2 bearing this missense mutation exhibits a 50–55% reduction in V_{max} when expressed in *Escherichia coli* (Sakowski *et al.* 2006*a*), PC12 cells (Zhang *et al.* 2004), or natively in the brain (Zhang *et al.* 2004; Cervo *et al.* 2005; Isles *et al.* 2005). The segregation of the alleles 1473C and 1473G in the brain of a number of inbred mouse strains has now been demonstrated by several groups (Zhang *et al.* 2004; Cervo *et al.* 2005; Crowley *et al.* 2005; Isles *et al.* 2005; Kulikov *et al.* 2005, 2007; Izikki *et al.* 2007). Polymorphism at this single locus has been associated with differences in aggressive behaviours (Kulikov *et al.* 2005; Popova, 2006), cardiac hypertrophy (Izikki *et al.* 2007), pre-mRNA editing of 5-HT_{2C} receptors (Englander *et al.* 2005; Hackler *et al.* 2006), and response to antidepressants (Cervo *et al.* 2005; Calcagno *et al.* 2007). This accounts for the majority of variation in 5-HT synthesis between inbred mouse strains (Kulikov *et al.* 2007).

We hypothesized that enteric neurones from inbred mouse strains also express polymorphic *tph2*, and that the resulting difference in neural 5-HT synthesis would correlate with functional outcomes in 5-HT-mediated motility patterns, permitting the role of 5-HT released from enteric nerves to be deduced by inter-strain comparisons. In this study, genetic, anatomical and functional methods were used to test this hypothesis. Preliminary results have been communicated (Neal & Bornstein, 2007*b*, 2008*a*; Neal *et al.* 2008).

Methods

Ethical approval

Ethical approval for these experiments was given by The University of Melbourne Animal Experimental Ethics Committee in accordance with the Australian Code of Practice for the Care and Use of Animals for Scientific Purposes.

Animals

C57Bl/6JArc (C57Bl/6) mice and Balb/cJArc (Balb/c) mice were obtained from the Animal Research Centre (Canning Vale, WA, Australia) and maintained on-site by the Biological Research Facility in the Departments of Physiology and Pharmacology at The University of Melbourne. Only adult males ($>$ 17 g, 6–8 weeks old) were used. Mice for use in genetic studies were killed by CO_2 asphyxiation to preserve the integrity of the brainstem for dissection; all other mice were killed by cervical dislocation. Subsequent procedures were carried out *in vitro*.

Genetic studies

Tissue preparation. Samples of brainstem, duodenum, jejunum and distal colon were removed from the animal and dissected on ice. Samples were bathed in sterile, iced phosphate-buffered saline (PBS; 0.01 M) throughout. Mucosa and circular muscle were quickly removed from the underlying longitudinal muscle–myenteric plexus (LM-MP) using sterile forceps, and discarded. All further processing of gut samples for standard and reverse transcriptase- (RT-) PCR work was performed on LM-MP samples alone.

Genomic DNA extraction. DNA was isolated from gut tissue homogenized in 100 μl NaOH (25 mM) and EDTA (0.2 mM), incubated at 95°C for 45 min, and buffered with Tris-HCl (40 mM, pH 5.0). Samples were centrifuged at 9391 g at room temperature for 2 min. The supernatant was taken for standard PCR.

Standard PCR. The expression of *tph2* polymorphism C1473G was assessed in genomic DNA from Balb/c and C57Bl/6 mice using standard PCR as previously described (Zhang *et al.* 2004). All standard PCR was performed in a Mastercycler Gradient machine (Eppendorf AG, Hamburg, Germany). Each 20 μl PCR reaction consisted of (μl): sterile H_2O (15.7); 10$\times$ pre-mixed reaction buffer with 10 M MgCl (2); 10 mM deoxyribonucleotide triphosphate (dNTP) mix (0.5); forward primer (0.2); control reverse primer (0.2); allele-specific reverse primer (either C or G, 0.2); EconoTaq (0.2); and template (1). Primers were obtained from Geneworks Pty Ltd (Hindmarsh, SA, Australia); EconoTaq DNA polymerase was obtained from Lucigen Corp. (Middleton, WI, USA); dNTP mix and pre-mixed reaction buffer were obtained from Scientifix Pty Ltd (Cheltenham, VIC, Australia). Sterile water was used as a negative control. PCR products (3 μl) were resolved by gel electrophoresis on 0.5% TBE agarose gels with ethidium bromide (Invitrogen Australia Pty Ltd, Mount Waverley, VIC, Australia). A 100 bp

TrackIt DNA ladder (Invitrogen) was used to estimate PCR product size. Gels were photographed using the UVP BioDoc-IT System (2UV Transilluminates; Pathtech Pty Ltd, Box Hill, VIC, Australia).

RNA extraction. Total RNA was isolated from gut and brainstem tissues homogenized in 1 ml of TRI Reagent (Ambion; Applied Biosystems, Scoresby, VIC, Australia). Chloroform (0.2 ml v/v) was added to the homogenate and incubated for 10 min. Samples were centrifuged at 12 000 *g* (4°C) for 15 min. The aqueous phase was transferred into a clean tube, with 0.5 ml isopropanol, and incubated at room temperature for 15 min. Samples were centrifuged at 12 000 *g* (4°C) for 15 min to precipitate the RNA. The RNA pellets were washed in 1 ml 75% ethanol and centrifuged for 5 min. After removing all traces of ethanol, samples were air dried and resuspended in RNASecure water (Ambion). The concentration of RNA in each sample was measured using a NanoDrop ND-1000 Spectrophotometer (Biolab Australia Pty Ltd, Clayton, VIC, Australia). RNA integrity was analysed on a 1% 0.5× TBE agarose gel with 1.5 μl SYBR Safe DNA gel stain (Invitrogen) to demonstrate the presence of ribosomal RNA bands (18S and 28S). Between 4 and 8 μg RNA was then incubated with 1 U DNase I (Ambion) at 37°C for 20 min to remove potential contaminating genomic DNA before cDNA synthesis.

First strand cDNA synthesis. First strand cDNA synthesis used 1 μg total RNA in a 20 μl reaction mix which contained 1 μl dNTP mix (10 mM), 1 μl random hexamers (0.5 μg μl^{-1}; Bioline, Alexandria, NSW, Australia) or 1 μl oligo(dT) 12–18 (0.5 μg μl^{-1}; Invitrogen) and nuclease-free water (Promega, Annadale, NSW, Australia). Samples were incubated at 65°C for 5 min and transferred to ice for 1 min. Each sample was supplemented with 4 μl of 5× First Strand buffer (Invitrogen), 1 μl of 0.1 M dTT (Promega), 1 μl of RNase inhibitor (400 U μl^{-1}; Promega) and incubated at room temperature for 2 min. One microlitre of Superscript III reverse transcriptase (200 U μl^{-1}; Invitrogen) was added and incubated at room temperature for 5 min. Samples were first incubated at 50°C for 60 min and then at 70°C for 15 min to terminate the reaction.

RT-PCR. The expression of the *tph2* C1473G polymorphism was assessed in brain and gut cDNA from Balb/c and C57Bl/6 mice using RT-PCR. Oligonucleotide primers were the same as for standard PCR, with the omission of the control reverse primer (Zhang *et al.* 2004). All RT-PCR was performed in the GeneAmp PCR system 2700 (Applied Biosystems). Each 20 μl reaction mix consisted of 10 μl GoTaq Green Master Mix (Promega), 5.6 μl nuclease-free water, 1.2 μl TPH2 forward and 1.2 μl of either the G-allele or C-allele reverse oligonucleotide primer (20 μm), and 2 μl cDNA template. Genomic DNA from each of the inbred strains was included as a positive control. One PCR reaction contained water instead of a cDNA template as a negative control. The PCR conditions were as follows: 1 cycle (94°C, 5 min) and then 40 cycles (94°C, 30 s, 60°C, 1 min, 72°C, 1 min) with a final extension at 72°C for 10 min. PCR products (10 μl) were resolved by gel electrophoresis on 2% TBE agarose gels with 15 μl SYBR Safe (Invitrogen). The DNA marker HyperLadder IV (Bioline) was used to estimate PCR product size. Gels were photographed using the UVP BioDoc-IT System (Pathtech). The identity of the PCR product was verified by nucleotide sequencing.

Anatomical studies

Immunohistochemistry. Segments (3–5 cm) of jejunum were removed from mice of both strains. Preliminary results indicated that the established pre-loading method of 5-HT visualization (Wardell *et al.* 1994; Young & Furness, 1995; Neal & Bornstein, 2007*a*) produced faint staining in tyrosine hydroxylase (TH) -immunoreactive (-IR) teminals, but a newer method described by Chen *et al.* (2001) did not. All further experiments were therefore performed using the latter method with some minor modifications. Samples were collected in PBS with 2.5 μM nicardipine (Sigma-Aldrich, Castle Hill, NSW, Australia) at 4°C to minimize 5-HT release from mucosa (Bertrand, 2006) and hence uptake by enteric neurones. Tissue was dissected into LM-MP preparations as described above and fixed in 4% paraformaldehyde–3% sucrose for 80 min at room temperature as described by Chen *et al.* (2001). Whole-mounts were processed for immunohistochemical identification of 5-HT-, and nitric oxide synthase (NOS)-, calretinin-, and/or TH-IR; antibodies are detailed in Tables 1 and 2. Whole-mounts were mounted in fluorescence mounting medium (Dako Australia Pty Ltd, Botany, NSW, Australia). The specificity of endogenous 5-HT labelling was confirmed by simultaneous processing for 5-HT- and TH-IR (Fig. 1).

Confocal microscopy. Images were collected and appositions quantified as previously described (Mann *et al.* 1997; Neal & Bornstein, 2007*a*, 2008*b*). Size factor was calculated for a randomly selected subset of NOS-IR neurones according to the method described by Neal & Bornstein (2007*a*). Calretinin-IR neurones were classified as Dogiel type II neurones if they had large, smooth cell bodies; normally more than one neurite could also be identified. All other calretinin-IR neurones were classified as 'non-Dogiel type II'.

Table 1. Primary antibodies used in this study

Antiserum	Specific immunogen	Host species	Dilution	Supplier	Catalogue	Reference
5-HT	5-HT coupled to bovine serum albumin with paraformaldehyde	Rabbit	1 : 2000	ImmunoStar Inc., Hudson WI, USA	20080 Lot 541317	(Chen *et al.* 2001)
Calretinin	Human recombinant calretinin	Goat	1 : 1000	Swant, Bellinzona, Switzerland	CG1 Lot 1§.1	(Sharkey *et al.* 1998)
NOS	Neuronal NOS	Sheep	1 : 1000	Gift of P. Emson, Cambridge, UK	K205	(Williamson *et al.* 1996)
TH	Native TH from rat phaeochromocytoma	Sheep	1 : 160	Chemicon, North Ryde NSW, Australia	AB1542 Lot 25020624	(Haycock & Waymire, 1982)
TH	Synthetic peptides from human and mouse TH	Chicken	1 : 100	Chemicon	AB9702 Lot 0605030481	

Table 2. Secondary antisera used in this study

Antiserum	Fluorophore	Host	Dilution	Supplier	Catalogue
Chicken	Rhodamine	Donkey	1 : 400	Chemicon	AP194R
Goat	Alexa 594	Donkey	1 : 200	Molecular Probes, Mt Waverley VIC, Australia	A11058
Rabbit	Alexa 488	Donkey	1 : 200	Molecular Probes	A21206

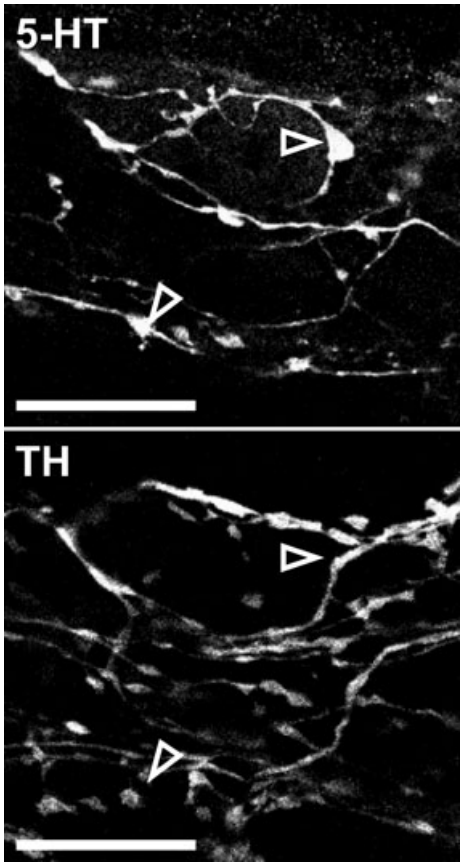

Figure 1. Endogenous 5-HT labelling is specific
Corresponding images of 5-HT- and TH-IR from the same field of view show no overlap between labels. Open arrows indicate example 5-HT-IR varicosities which are not visible in the corresponding TH image. These images were constructed by merging 2 consecutive layers from a z-series. Scale bars, 20 μm.

Statistical analysis

Anatomical data are presented as mean ± standard error of the mean (S.E.M.) apposed varicosities unless specified. N is the number of neurones examined. Data were compared between strains using unpaired t tests and significance was set at $P < 0.05$.

Functional studies

Tissue preparation. Segments of jejunum (4–7 cm) were removed from mice of each strain and placed in organ baths each containing 15 ml of warmed (36°C) physiological saline solution (composition, mM: NaCl 118, KCl 4.6, NaH_2PO_4 1, $NaHCO_3$ 25, $MgSO_4$ 1.2, D-glucose 11, $CaCl_2$ 2.5; bubbled with 95% O_2 : 5% CO_2). Each tissue served as its own control. Physiological saline was continuously superfused through the organ bath at a flow rate of approximately 6 ml min^{-1}. Segments were connected to an adjustable pressure head via oral and anal cannulae, as previously described (Gwynne *et al.* 2004); intraluminal pressures were maintained at 5–6 cmH_2O. Preliminary data indicate that these pressures are required for the establishment of regular PCCs (L. L. Tan, unpublished data); slightly lower pressures have been used in murine jejunum by other groups (Abdu *et al.* 2002). After cannulation, tissue was left to equilibrate for 40 min.

Experimental protocol. PCCs were defined as contraction complexes that propagated in a consistent direction for 50% or more of the length of the gut segment. Following equilibration, time controls were performed

on jejunal segments from eight Balb/c and six C57Bl/6 mice to determine the time over which PCCs were consistent under the conditions of these experiments. Frequency of PCCs was used as an index of consistency. In C57Bl/6 tissues, frequency remained constant over the entire recording period of up to 3 h. However, PCC frequency in Balb/c fell from about 0.55 min^{-1} to $< 0.3\ min^{-1}$ over this period (Fig. 2), although this was not statistically significant due to a large variance. As a result, the experimental protocol was designed so that recordings would normally be completed within 80 min of equilibration: video images were recorded for 20 min in control, drug and washout conditions. A non-recording interval of 20 min was observed for washout of drugs from the bath. In some experiments, TTX (1 μM; Laboratories, Jerusalem, Israel) was added for 10 min following drug application and prior to washout, to determine if any of the observed effects were due to direct actions on the smooth muscle. Washout data were extremely variable and are not reported here.

Drugs. All drugs used in these experiments were applied to the superfusate. Drugs used included TTX (1 μM), the 5-HT_3 receptor antagonist, granisetron (1 μM), and the 5-HT_4 receptor antagonist, SB207266 (10 nM; both kind gifts from SmithKline Beecham, Australia). Granisetron and SB207266 were applied either alone or in combination. All drugs were initially made up in distilled water to form stock solutions. Final concentrations of drug were achieved by diluting stock in the superfusing saline and simultaneously adding titrated stock directly to the bath to bring the local concentration quickly to the desired level. Video recordings of drug conditions began within 2 min of addition of drug stock solutions to the bath.

Video imaging. Spatio-temporal maps were constructed using in-house software from video recordings taken with a Logitech camera (QuickCam Pro 4000; I-Tech, Ultimo, NSW, Australia) mounted directly above the organ bath as previously described (Gwynne *et al.* 2004; Roberts *et al.* 2007, 2008). Raw maps showed low-frequency and high-frequency oscillating contraction components (Fig. 3). Fast Fourier transform indicated that the high-frequency oscillations had a frequency (Balb/c, 0.74 ± 0.02 Hz, $n = 4$; C57Bl/6, 0.74 ± 0.03 Hz, $n = 4$) that resembled slow waves in jejunum (L. L. Tan, unpublished data; Seerden *et al.* 2005). These were unaffected by TTX (Fig. 3*Cb*), indicating that they were not neurogenic, and preliminary data showed that they occurred in phase with slow waves at any given recording site (R. R. Roberts, unpublished data). In contrast, the low-frequency component was blocked by TTX (Fig. 3*C* and *D*). Accordingly, the high-frequency oscillatory activity (> 0.1 Hz) was filtered from the raw spatio-temporal maps, so that final maps represented only neurally dependent activity.

Parameters and statistics. PCC parameters extracted from spatio-temporal maps included: frequency (min^{-1}), period (s), amplitude (% of resting gut width), duration (s), quiescence (s), velocity ($mm\ s^{-1}$) and number of contraction peaks per complex, among others (Fig. 4). Velocity was defined as 'positive' when PCCs propagated anally. Frequency was calculated as PCCs per minute in a given 20 min spatio-temporal map. Velocity was calculated from spatio-temporal maps as the gradient of the PCC wavefront. Other variables were calculated from 2-dimensional extracts from spatio-temporal maps showing gut width over time, as illustrated in Fig. 4. Preparations were excluded from analysis if control activity was absent or irregular, e.g. wavefronts that were disrupted or propagated in more than one direction. Where PCCs were abolished or converted to irregular activity in drug conditions, all parameters except period and quiescence were entered as 0, while mean period and quiescence were entered as 1200 s, a theoretical maximum based on the duration of recording. PCCs were taken to be abolished by drug(s) only if organized activity reappeared after washout. Data are reported as means ± S.E.M. Effects of drugs within strains were analysed by paired *t* tests. Where PCCs were abolished in drug conditions, two proportion tests between strains were performed on the number of affected preparations. *N* is the number of animals from which measures were taken, and significance was set at $P < 0.05$.

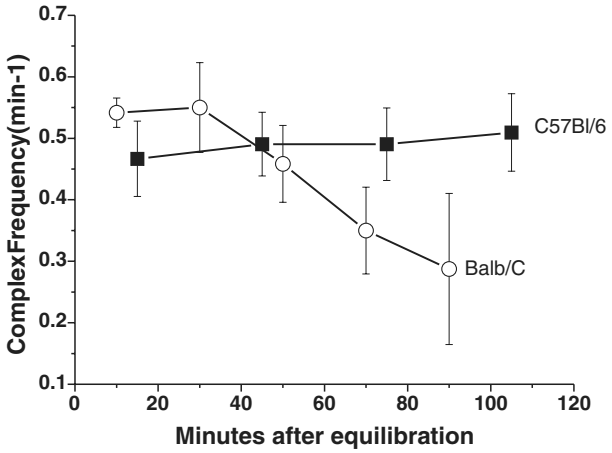

Figure 2. Frequency of PCCs during time controls
Balb/c (○, $n = 8$) and C57Bl/6 (■, $n = 6$) in jejunum. Frequency of PCCs tended to be more stable in C57Bl/6 mice over time than in Balb/c mice. Frequency in jejunum from Balb/c mice tended to decrease over the period of recording, but this did not reach statistical significance ($P > 0.05$, ANOVA, Tukey's *post hoc* test).

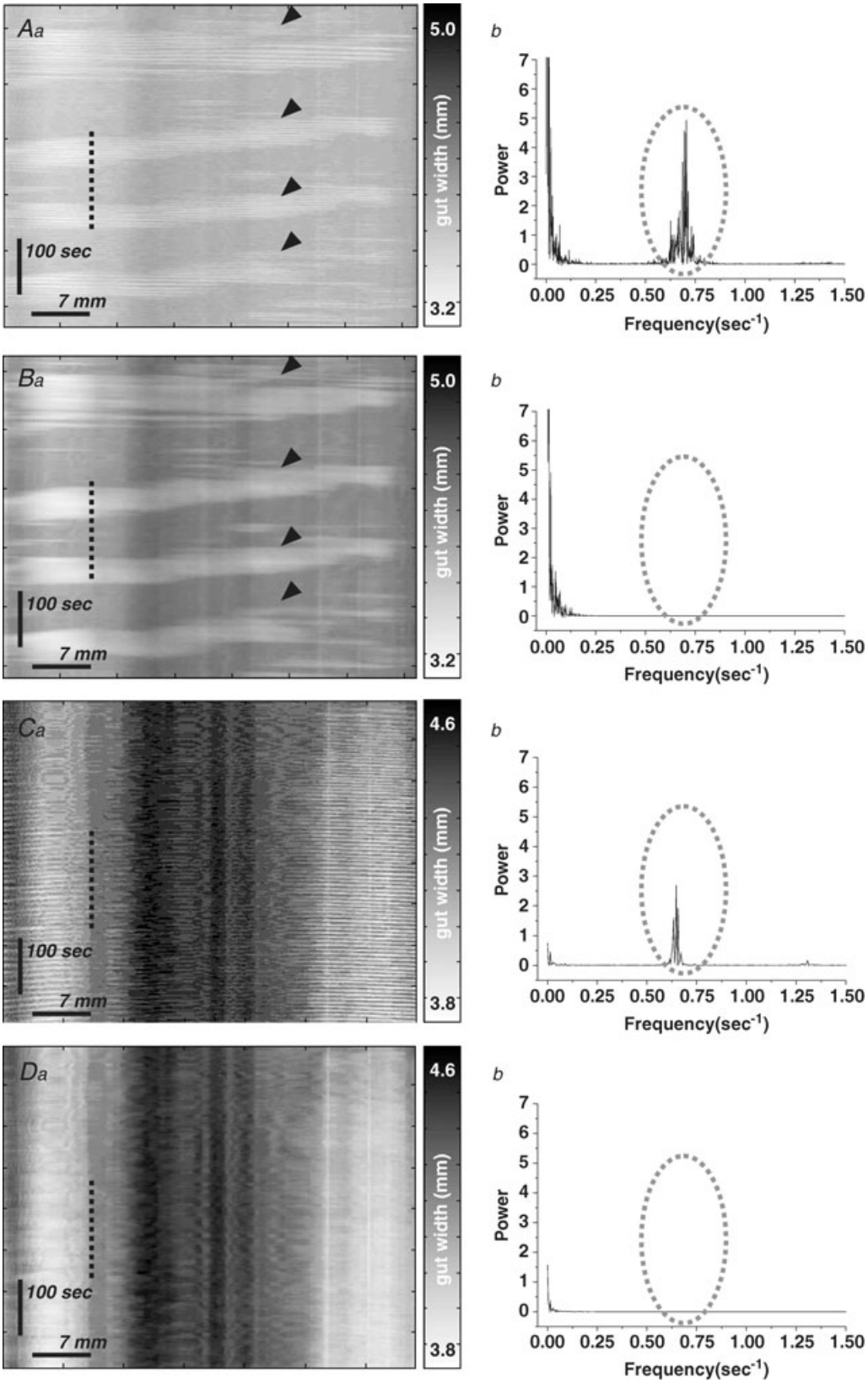

Figure 3. Two types of contraction are revealed by spatio-temporal maps of adult mouse intestine *in vitro*

Aa–Da, spatio-temporal maps showing contractile activity of murine jejunum in control (*A–B*) and TTX (*C–D*). In control maps, low frequency propagating contractions (PCCs) can clearly be seen (*Aa*, arrowheads), but fast

Pharmacological studies

Longitudinal segments of jejunum were suspended in 6 ml organ baths containing physiological saline and attached to isotonic transducers (SDR Technology, Sydney, NSW, Australia) with a resting tension of 0.3 g. The bathing physiological saline was maintained at 36.5°C and bubbled continuously with 95% O_2−5% CO_2. Segments were equilibrated for 1 h with changes of physiological saline every 10–15 min. Contractile responses were recorded on to a PC hard drive using a Biopac M100A (SDR Technology) with a sampling rate of 10 s^{-1}. Data were analysed using Acqknowledge 3.2.4 software (SDR Technology). Initially, carbachol (muscarinic agonist, 10 μM) was added to the organ bath to elicit near-maximal contractions; subsequent measurements in each segment were normalized to this contraction. All drugs were washed out of the specimen by three to four complete changes of physiological saline over a 5 min period, and the tissue was allowed to recover for 15 min before further intervention. In concentration–effect experiments, segments from each animal were exposed to exogenous 5-HT (10 or 100 μM) alone, and then following a 15 min incubation in TTX (1 μM). In a parallel series of experiments, the 5-HT_1 and 5-HT_2 antagonists methiothepin (100 nM) and ketanserin (30 nM) were added to the superfusing saline from the beginning of the experiment. In this second series of experiments, segments of jejunum were exposed to 5-HT (10 μM) alone, and then after 15 min incubation in granisetron (1 μM) or combined granisetron and SB207266 (10 nM). Carbachol was reapplied at the end of all experiments to demonstrate the continuing viability of the muscle.

Data are expressed as a per cent of the initial carbachol response (mean ± S.E.M.). N is the number of animals. Data were analysed by two-way ANOVA or t test as appropriate.

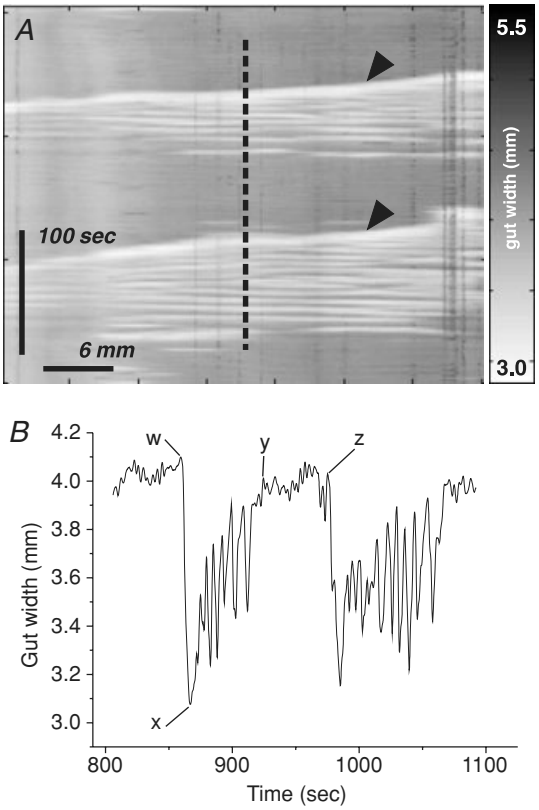

Figure 4. Measurement of PCC parameters
A, frequency (min^{-1}) and velocity (gradient, mm s^{-1}) of PCCs (arrowheads) were measured from spatio-temporal maps directly. Speed was the absolute value of the velocity. Other parameters were calculated from 2-dimensional plots of time and gut width extracted from spatio-temporal maps at a consistent point along the *x*-axis. The plot in *B* derives from the dashed line in *A*; the alphabetically labelled points were used to calculate additional parameters as follows: Amplitude = 100((w – x)/w); Duration = y – w; Period = z – w; Quiescence = z – y; Inhibition ratio = (z – y)/(z – w). Contractions/PCC was the number of peaks between points w and y. These points were defined as follows: x is the point of maximum contraction in a complex; w and z are the points of inflection from baseline on rising phase of consecutive contractions; y is the point of inflection to baseline on the falling phase of a contraction. Parameters were calculated from all PCCs in each spatio-temporal map, and averaged between animals.

Results

tph2 Genotype and mRNA expression

Genomic DNA. The *tph2* polymorphism C1473G was strain-specifically expressed in Balb/c and C57Bl/6 mice in accordance with previous reports (Zhang *et al.* 2004). Three of three Balb/c mice homozygously expressed the G allele, while 4 of 4 C57Bl/6 mice homozygously expressed the C allele (Fig. 5*A* and *C*).

mRNA expression. mRNA encoding the high-activity enzyme TPH2 (C/C) was detected in LM-MP samples from jejunum, colon and brainstem of C57Bl/6, but not Balb/c, mice (Fig. 5*B*). In contrast, mRNA encoding the low-activity enzyme TPH2 (G/G) was detected in similar samples, plus the duodenum, of Balb/c, but not C57Bl/6, mice (Fig. 5*D*). In both cases, the allele-specific

Fourier transform also reveals a high frequency peak at 0.70–0.75 Hz (*Ab*, dotted area). Low-pass filtering removes this high frequency element (*Bb*, dotted area), without affecting the appearance of PCCs (*Ba*, arrowheads). Low, but not high frequency activity is abolished by TTX (*Ca* and *b*). Low-pass filtering removes the high frequency activity from TTX maps (*Da* and *b*).

PCR product of approximately 180 bp was expressed only in cDNA from gut and brain tissues (and not the genomic DNA), suggesting this was TPH2 mRNA. The allele-specific 300 bp PCR product was strongly expressed in the genomic DNA samples and also in the gut mRNA samples. This is similar to the 307 bp product previously reported in genomic DNA (Zhang *et al.* 2004; Cervo *et al.* 2005). The lack of TPH2 mRNA in the duodenum in most of the samples was most likely due to RNA degradation, confirmed by the absence of PCR products for the housekeeping gene *gapdh* (data not shown). It should be noted that these samples expressed the allele-specific

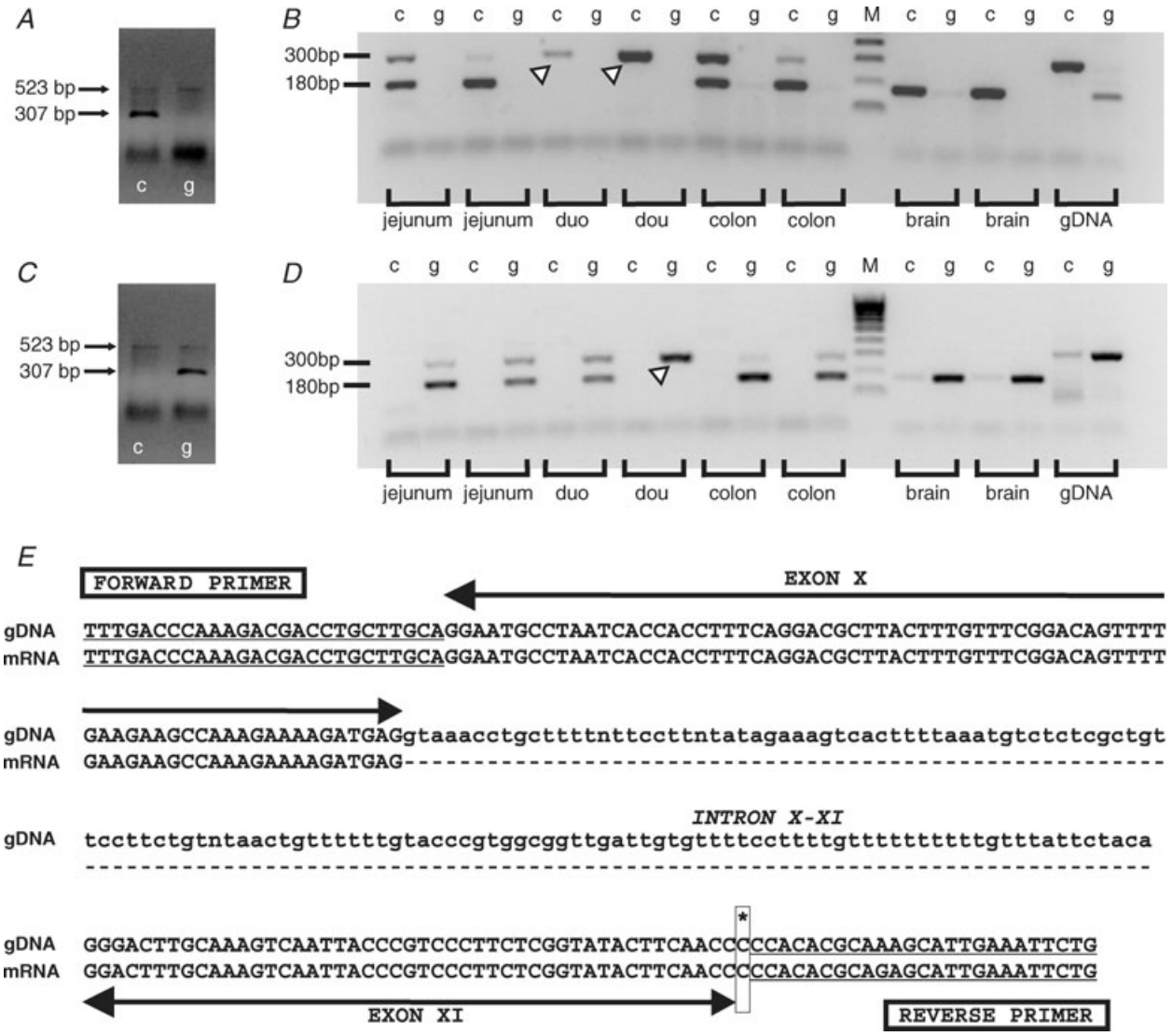

Figure 5. Expression of tph2 C1473G polymorphism is strain specific
Standard PCR revealed allele-specific PCR products of approximately 300 bp for the C allele only in C57Bl/6 mice (*A*), while products for the G allele were only observed in Balb/c mice (*C*). The faint 523 bp control product can be seen faintly in each lane of *A* and *C*, indicating that the reactions were successful. mRNA encoding the high-activity enzyme TPH2 (C/C) was detected as a 180 bp RT-PCR product only in tissues from C57Bl/6 mice (*B*). mRNA encoding the low-activity enzyme TPH2 (G/G) was detected by RT-PCR in similar samples only in Balb/c mice (*D*). RNA degradation resulted in a lack of TPH2 mRNA in most duodenum samples. However, these samples expressed allele-specific 300 bp PCR products in the genomic DNA samples (arrowheads). Sequence analysis on PCR products from C57Bl/6 mice confirmed that the 180 bp PCR product consists of 101 nucleotides in exon X and 73 in XI of the TPH2 gene, whereas the larger 300 bp PCR product also includes 130 nucleotide sequence of intron X–XI (*E*). Sequencing could not confirm the allele at nucleotide position 1473 (asterisk and box) because of the primer binding at this location. Key: c, lanes showing PCR products from the c-allele-specific reactions; g, lanes showing PCR products from the g-allele-specific reactions; M, reference DNA ladder.

300 bp PCR products, showing that genomic DNA was present. In summary, gene transcripts encoding TPH2 isoforms were strain-specifically expressed in myenteric neurones of murine jejunum and colon, and also in the brain.

Sequence analysis. Nucleotide sequence analysis confirmed that the 180 bp PCR product consisted of nucleotides in exon X and X1 of the TPH2 gene, whereas the larger 300 bp PCR product included the sequence of intron X–X1, as well as exon X and X1 (Fig. 5*E*).

Immunohistochemistry of myenteric plexus

Jejuna from 12 mice (5 Balb/c; 7 C57Bl/6) were processed for immunohistochemical visualization of endogenous 5-HT and other markers. Results are illustrated in Fig. 6, and quantitative data are presented in Fig. 7.

Specificity of 5-HT labelling. Specificity of 5-HT labelling was tested in 38 z-series (field of view 90 μm × 90 μm) through the centre of ganglia from four Balb/c mice, and 33 z-series from four C57Bl/6 mice, double-stained with antibodies raised against 5-HT and TH (Fig. 1). Overlap was measured using Pearson's correlation coefficient (R), calculated in ImageJ V1.63 freeware for Windows (Wayne Rasband, National Institute for Mental Health, Bethesda, MD, USA; http://rsb.info.nih.gov/ij/index.html), for 36 focal planes from C57Bl/6 mice and 44 focal planes from Balb/c mice selected at random from the above z-series. Mean R approached zero in both strains (Balb/c, -0.07 ± 0.01; C57Bl/6, -0.05 ± 0.01), indicating that TH- and 5-HT-IR were independently distributed.

5-HT–NOS connection patterns. Rings of 5-HT-IR varicosities were sometimes observed in jejunum, but never surrounding NOS-IR cell bodies (Fig. 6*A*–*D*). Very few 5-HT-IR varicosities were found in apposition to NOS-IR neurones in jejunum of either strain (Balb/c: 0.9 ± 0.2, $n = 78$; C57Bl/6: 1.6 ± 0.3, $n = 52$). NOS-IR neurones in Balb/c mice were apposed by significantly fewer 5-HT-IR varicosities than those in C57Bl/6 mice (Student's t test, $P < 0.05$; Fig. 7*A*), and a significantly greater proportion of NOS-IR neurones examined in Balb/c mice was not apposed by any 5-HT-IR varicosities (Balb/c: 46/78, 59%; C57Bl/6: 20/52, 38%; 2-proportion test, $P < 0.04$; Fig. 7*B*). The size of 15 Balb/c and 15 C57Bl/6 NOS-IR neurones randomly selected from the above data was estimated. Size of NOS-IR neurones in Balb/c jejunum ranged from 147 to 500 μm^2, with a mean size of 287 ± 28 μm^2. In C57Bl/6 jejunum, NOS-IR neurones ranged in size from 150 to 457 μm^2, with a mean size of 314 ± 25 μm^2. Mean size did not differ between strains ($P > 0.4$).

5-HT–calretinin connection patterns. Calretinin-IR cell bodies were frequently surrounded by rings of 5-HT-IR varicosities or apposed by calices of varicosities on one side (Fig. 6*E* and *F*). Jejunal calretinin-IR neurones from each strain were apposed by 3.5 ± 0.3 (Balb/c, $n = 98$) and 5.2 ± 0.4 (C57Bl/6, $n = 54$) 5-HT-IR varicosities. Mean numbers of 5-HT-IR varicosities apposed to calretinin-IR neurones were significantly larger in C57Bl/6 than Balb/c mice ($P < 0.01$, Fig. 7*C*). However, calretinin-IR neurones that were not apposed by 5-HT-IR varicosities were also observed in both strains (Balb/c: 20/98, 20%; C57Bl/6: 6/54, 11%; 2-proportion test, $P > 0.1$; Fig. 7*D*). When calretinin-IR neurones were categorized morphologically as Dogiel type II or non-Dogiel type II, mean apposed varicosities per Dogiel type II neurone were similar between strains, but apposed varicosities per non-Dogiel type II neurone were more numerous in C57Bl/6 mice than in Balb/c mice ($P < 0.05$, Fig. 7*E*). The frequency distributions for apposed 5-HT varicosities per Dogiel type II or non-Dogiel type II cell body in Balb/c and C57Bl/6 mice resembled each other (Fig. 7*F* and *G*), and in both strains some cell bodies of both Dogiel type II (Balb/c: 7/20, 35%; C57Bl/6: 2/13, 15%, $P > 0.7$) and non-Dogiel type II (Balb/c: 13/78, 17%; C57Bl/6: 4/41, 10%; 2-proportion test, $P > 0.2$) neurones were not apposed by any 5-HT-IR varicosities. High numbers (> 10) of varicosities were seen in apposition to a small number of Dogiel type II neurones ($n = 2$) in C57Bl/6 mice only (Fig. 7*F*).

Other connection patterns. 5-HT-IR cell bodies were occasionally observed in each strain. Fainter somatic labelling of 5-HT-IR in comparison to varicosities allowed 5-HT-to-5-HT connectivity to be assessed in a small number of neurones (Balb/c, $n = 6$; C57Bl/6, $n = 5$). TH-IR connectivity was also examined in these neurones. Large numbers of 5-HT-IR (Balb/c, 24.7 ± 4; C57Bl/6, 21.4 ± 3) and TH-IR (Balb/c, 21.5 ± 2; C57Bl/6, 18.8 ± 2) varicosities were observed in apposition to each cell body (Fig. 6*G* and *H*). The numbers of TH-IR and 5-HT-IR varicosities apposed to each cell were similar (paired t test, $P > 0.4$, Fig. 7*H*). Mean numbers of 5-HT- and TH-IR varicosities apposed to 5-HT-IR cell bodies were significantly larger than the mean number of 5-HT-IR varicosities apposed to either calretinin- or NOS-IR cell bodies in both strains ($P < 0.01$). TH-IR varicosities also apposed both calretinin-IR (Fig. 6*I*) and NOS-IR (Fig. 6*J*) cell bodies, but these appositions were not quantified.

PCC activity in jejunum

Jejuna were removed from 20 Balb/c and 27 C57Bl/6 mice. Raw data in control and drug conditions are presented in Table 3, and discussed more fully below. The jejunal

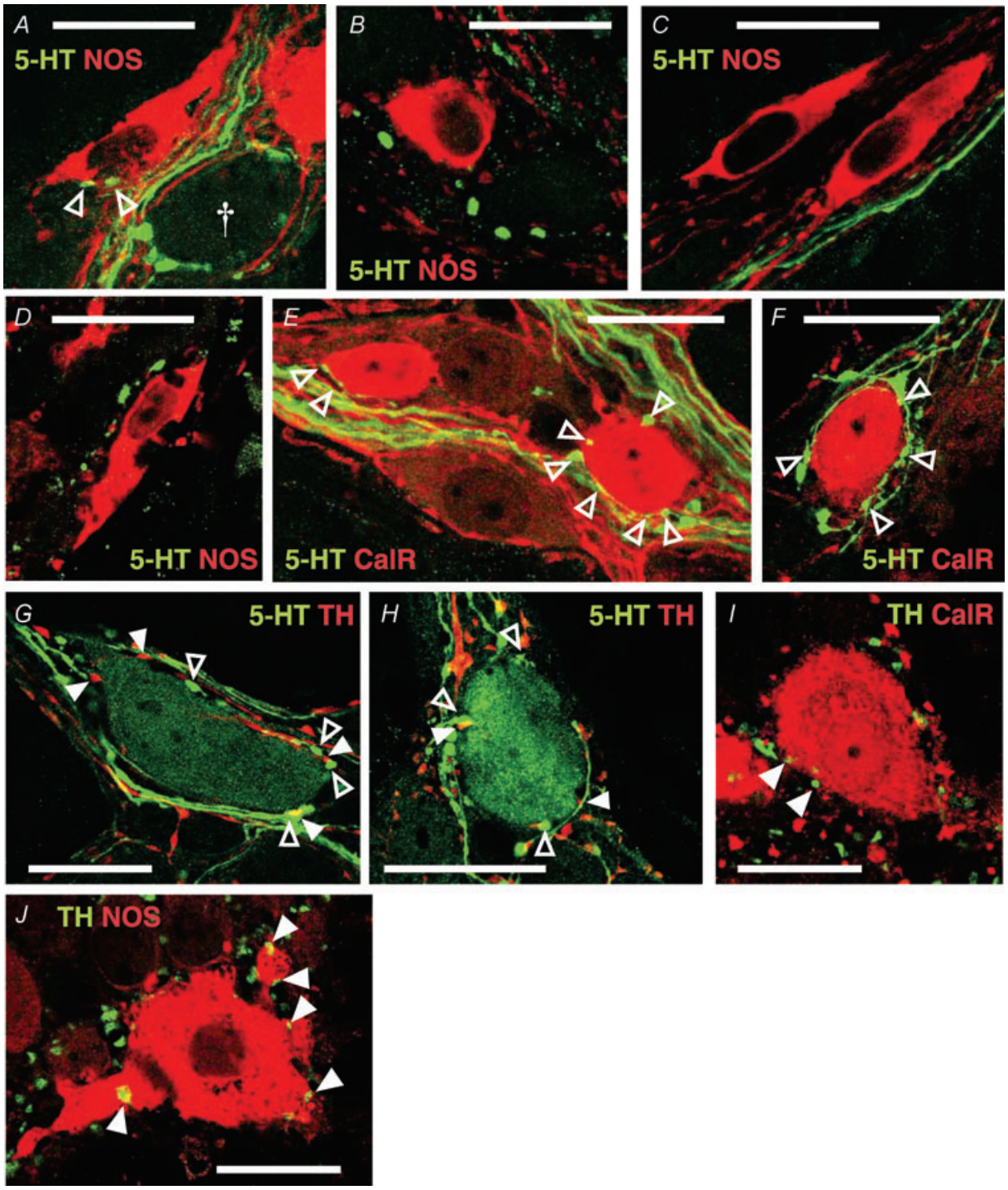

Figure 6. 5-HT and TH connections to jejunal neurones
A–D. 5-HT-IR (green) varicosities apposed to NOS-IR (red) cell bodies (open arrowheads) were extremely rare in both Balb/c (*A* and *B*) and C57Bl/6 (*C* and *D*) mice. Occasionally rings of 5-HT-IR varicosities were observed surrounding NOS^{-ve} cell bodies (*A*, †), but never surrounding NOS-IR cell bodies. Many NOS-IR neurones were not apposed by any 5-HT-IR varicosities (*B–D*). *E* and *F*, 5-HT-IR varicosites in apposition to calretinin-IR (red) neurones were relatively abundant in jejunum samples from both strains. Calices of varicosities arising from passing 5-HT-IR axons (*E*) were often seen in apposition to calretinin-IR cell bodies. Rings (*F*) of 5-HT-IR varicosities were also frequently observed surrounding calretinin-IR cell bodies. *G* and *H*, 5-HT-IR cell bodies were apposed by numerous 5-HT-IR and TH-IR (red, filled arrowheads) varicosities in Balb/c (*G*) and C57Bl/6 (*H*) jejunum. *I* and *J*, TH-IR varicosities (green) were observed in apposition to both calretinin-IR (red, *I*) and NOS-IR (red, *J*) cell bodies (filled arrowheads) in jejunum. These images were constructed by merging 1–3 planes from z-series. Scale bars, 20 μm.

PCC normally propagated in the oral direction (mean velocity: Balb/c, -0.4 ± 0.3 mm s^{-1}, $n = 20$; C57Bl/6, -0.7 ± 0.5 mm s^{-1}, $n = 27$). Control PCC frequency was significantly higher in Balb/c (0.59 ± 0.05 min^{-1}) than C57Bl/6 (0.45 ± 0.03 min^{-1}) mice, and duration (Balb/c, 58.5 ± 6.3 s; C57Bl/6, 81.6 ± 8.1 s) and interval (Balb/c, 105.2 ± 12.4 s; C57Bl/6, 143.8 ± 11.6 s) were correspondingly higher in C57Bl/6 mice ($P < 0.05$). Other control parameters did not differ significantly between strains. TTX abolished jejunal PCCs in all Balb/c ($n = 8$) and C57Bl/6 ($n = 8$) preparations.

Effects of granisetron. Tissue from eight Balb/c and nine C57Bl/6 mice was used to investigate the effects of granisetron on PCCs. Following the addition of granisetron, PCC parameters were not affected in Balb/c mice ($n = 8$, see Table 3A; Fig. 8). In C57Bl/6 mice, however, frequency decreased from 0.56 ± 0.1 min^{-1} to 0.33 ± 0.1 min^{-1} ($n = 9$, $P < 0.05$; see Table 3A, Fig. 8*C*) while amplitude decreased from $12 \pm 2\%$ resting gut width to $7 \pm 2\%$ resting gut width ($P < 0.05$, Fig. 8*D*). All contractions in granisetron were abolished by TTX application (Balb/c, $n = 5$; C57Bl/6, $n = 6$).

Effects of SB207266. Tissue from six Balb/c and eight C57Bl/6 mice was used to investigate the effects of SB207266 on PCCs. Mean velocity in both strains became positive following SB207266 application (Table 3B), but

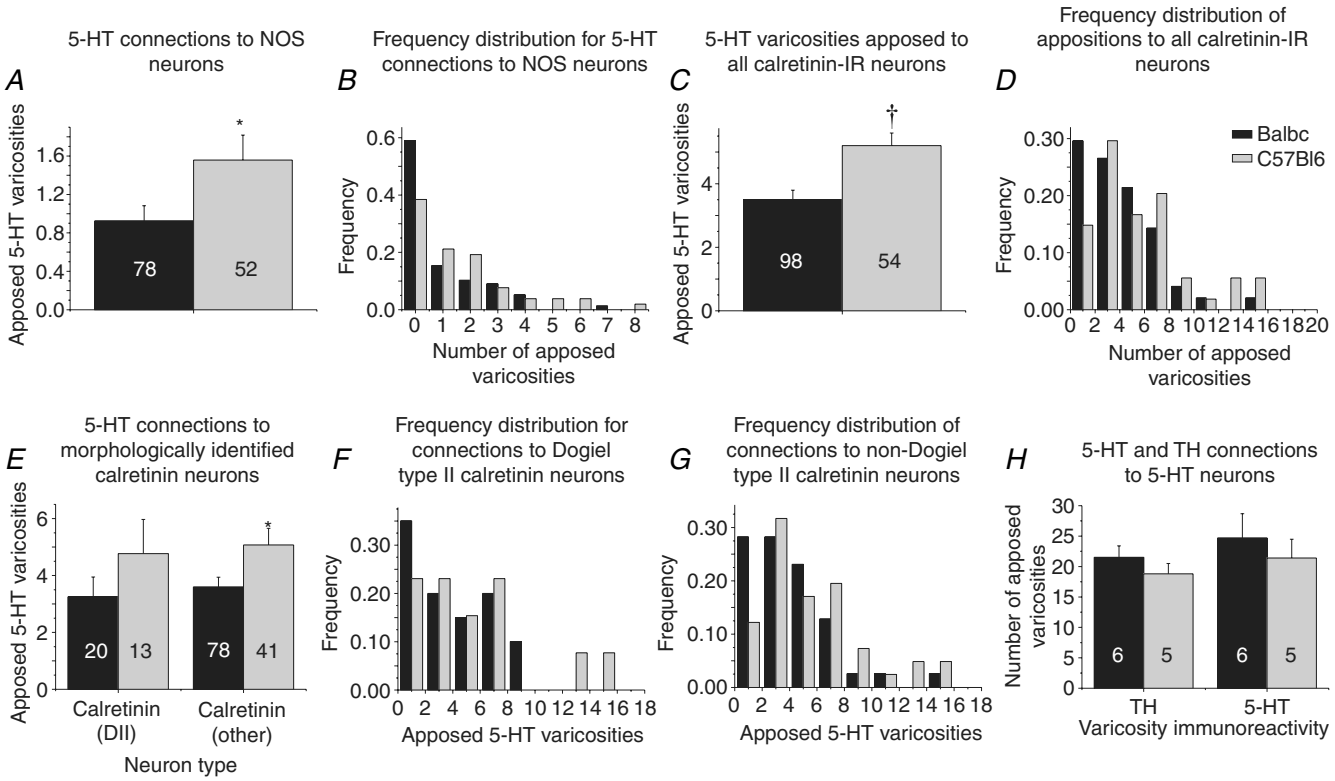

Figure 7. Quantified 5-HT and TH connections to jejunal neurones
A, mean numbers of 5-HT-IR varicosities apposed to NOS-IR cell bodies were significantly larger in C57Bl/6 mice. *B*, this difference is reflected in the frequency distribution of appositions per NOS-IR neurone. *C*, calretinin-IR cell bodies in C57Bl/6 mice were apposed by significantly greater numbers of 5-HT-IR varicosities than Balb/c. *D*, frequency distribution of appositions per neurone revealed a trend for more calretinin-IR cell bodies in Balb/c than C57Bl/6 mice not to be apposed by 5-HT-IR varicosities, while larger numbers of varicosities tended to be observed apposing calretinin-IR neurones from C57Bl/6 mice. *E*, Dogiel type II (DII) and non-Dogiel type II (other) calretinin-IR neurones were apposed by 5-HT-IR varicosities in both strains. Calretinin-IR neurones of both morphologies in C57Bl/6 mice tended to be apposed by larger numbers of 5-HT varicosities than neurones in Balb/c mice, but this only reached significance in non-Dogiel type II neurones. *F*, the proportion of Dogiel type II neurones that were apposed by no 5-HT varicosities was higher in Balb/c than C57Bl/6 mice, and the maximum number of varicosities apposed to a Dogiel type II neurone from Balb/c mice (8) was lower than the maximum in C57Bl/6 mice (18). *G*, the proportion of non-Dogiel type II neurones that were apposed by no. 5-HT varicosities was also larger in Balb/c than C57Bl/6 mice. *H*, mean numbers of 5-HT- and TH-IR varicosities apposed to each cell body were similar between and within strains. $^*P < 0.05$; †$P < 0.01$ between strains.

Table 3. Functional parameters of jejunal PCCs in response to 5-HT3 and/or 5-HT4 antagonists

A. Granisetron, 1 μM

Jejunum	Balb/c ($n = 8$)		C57Bl/6 ($n = 9$)	
Treatment:	Control	Granisetron	Control	Granisetron
Frequency (min^{-1})	0.71 ± 0.1	0.56 ± 0.1	0.56 ± 0.1	0.33 ± 0.1*
Amplitude (%)	9 ± 2	8 ± 1	12 ± 2	7 ± 2*
Duration (s)	53.9 ± 3.5	56.8 ± 4.9	61.2 ± 6.0	57.5 ± 7.4
Quiescence (Q, s)	35.2 ± 10.8	44.0 ± 7.8	56.2 ± 14.4	315.3 ± 128.1
Period (I, s)	88.9 ± 13.1	101.1 ± 11.9	119.4 ± 16.7	373.1 ± 122.1
Inhibition ratio (Q/I)	0.33 ± 0.1	0.55 ± 0.1	0.42 ± 0.1	0.55 ± 0.1
Contractions/PCC	9.0 ± 1.0	9.3 ± 1.2	9.0 ± 0.9	10.5 ± 1.8
Speed (mm s^{-1})	1.5 ± 0.3	1.8 ± 0.8	3.3 ± 0.7	2.6 ± 0.7
Velocity (mm s^{-1})	-0.5 ± 0.9	-0.4 ± 0.2	0.3 ± 0.9	1.9 ± 0.2

B. SB207266, 10 nM

Jejunum	Balb/c ($n = 6$)		C57Bl/6 ($n = 8$)	
Treatment:	Control	SB207266	Control	SB207266
Frequency (min^{-1})	0.51 ± 0.04	0.38 ± 0.1	0.31 ± 0.04	0.28 ± 0.04
Amplitude (%)	10 ± 2	6 ± 2	13 ± 5	13 ± 4
Duration (s)	45.8 ± 10.6	51.4 ± 12.6	109.5 ± 22.7	73.6 ± 6.3
Quiescence (Q, s)	43.8 ± 10.8	259.5 ± 188.9	85.1 ± 15.2	113.2 ± 15.5
Period (I, s)	90.0 ± 18.8	310.0 ± 178.9	194.8 ± 25.0	187.2 ± 15.7
Inhibition ratio (Q/I)	0.44 ± 0.1	0.6 ± 0.1	0.44 ± 0.1	0.59 ± 0.1*
Contractions/PCC	10.4 ± 3.3	11.6 ± 2.5	25.8 ± 3.2	17.8 ± 2.5
Speed (mm s^{-1})	1.6 ± 0.6	1.2 ± 0.4	1.4 ± 0.2	2.5 ± 0.5
Velocity (mm s^{-1})	-0.8 ± 0.3	0.2 ± 0.4	-0.5 ± 0.5	0.03 ± 1.0

C. Combined antagonists

Jejunum	Balb/c (n = 6)		C57Bl/6 (n = 10)	
Treatment:	Control	Combined antagonists	Control	Combined antagonists
Frequency (min^{-1})	0.50 ± 0.1	0.39 ± 0.1	0.46 ± 0.1	0.09 ± 0.05†
Amplitude (%)	20 ± 5	14 ± 4	12 ± 2	4 ± 2*
Duration (s)	77.3 ± 16.2	78.3 ± 33.4	77.7 ± 6.6	19.0 ± 9.9†
Quiescence (Q, s)	65.9 ± 17.6	230.5 ± 194.2	47.6 ± 9.4	862.3 ± 172.0†
Period (I, s)	142.1 ± 30.0	315.9 ± 181.4	125.1 ± 10.4	881.0 ± 162.5†
Inhibition ratio (Q/I)	0.4 ± 0.1	0.4 ± 0.1	0.4 ± 0.04	0.9 ± 0.1†
Contractions/PCC	24.1 ± 5.7	17.0 ± 7.4	18.3 ± 1.5	4.1 ± 2.2†
Speed (mm s^{-1})	1.9 ± 0.4	1.1 ± 0.4	2.3 ± 1.0	0.1 ± 0.1
Velocity (mm s^{-1})	0.2 ± 0.5	-0.5 ± 0.5	-1.9 ± 1.0	-0.1 ± 0.1

Paired t test between treatments: *$P < 0.05$; †$P < 0.01$.

this difference was not statistically significant. Mean frequency and amplitude were not significantly affected by SB207266 in either strain. In C57Bl/6 mice only, the proportion of the time during which the tissue was quiescent in each PCC period (inhibition ratio, Table 3B) increased significantly from 0.44 ± 0.1 to 0.59 ± 0.1 ($P < 0.05$). This was the only parameter in either strain to exhibit a significant change upon the addition of SB207266 alone. All contractions in SB207266 were abolished by TTX (Balb/c, $n = 2$; C57Bl/6, $n = 2$).

Effects of combined antagonists. Tissue from 6 Balb/c and 10 C57Bl/6 mice was used to investigate the effects in jejunum of the combined 5-HT_3 and 5-HT_4 receptor antagonists. Application of combined antagonists to jejunum resulted in abolition of the PCC in a significantly higher proportion of C57Bl/6 (8/10, 80%) than Balb/c (1/6, 17%) preparations (2-proportion test, $P < 0.05$). Abolition of the PCC included complete abolition of contractile activity ($n = 4$, C57Bl/6 only), or conversion of PCCs to non-propagating irregular activity ($n = 1$, Balb/c;

$n = 4$, C57Bl/6, Fig. 9*A*). No significant changes in any parameters were detected in Balb/c mice, but frequency (Fig. 9*C*), amplitude (Fig. 9*D*), duration and contractions per PCC all decreased significantly in C57Bl/6 mice, while both quiescence and period significantly increased (Table 3C).

Pharmacology of 5-HT

Tissue from 10 Balb/c and 10 C57Bl/6 mice was used to test the sensitivity of jejunal segments to exogenous 5-HT in the presence and absence of a variety of 5-HT receptor antagonists and the neural activity blocker TTX (see Fig. 10 for data). No strain differences were observed when 5-HT was applied at 10 μM (t test, $P > 0.3$) or 100 μM (t test, $P > 0.5$; Fig. 10*B*). Responses in both strains were significantly reduced in the presence of TTX (paired t test, $P < 0.05$), but there was no significant difference between strains in the residual response (t test, $P > 0.1$; Fig. 10*B*). In the presence of methiothepin and ketanserin, the 5-HT-evoked response was significantly reduced in both strains (Balb/c from $62.4 \pm 7.3\%$ to $34.7 \pm 3.6\%$,

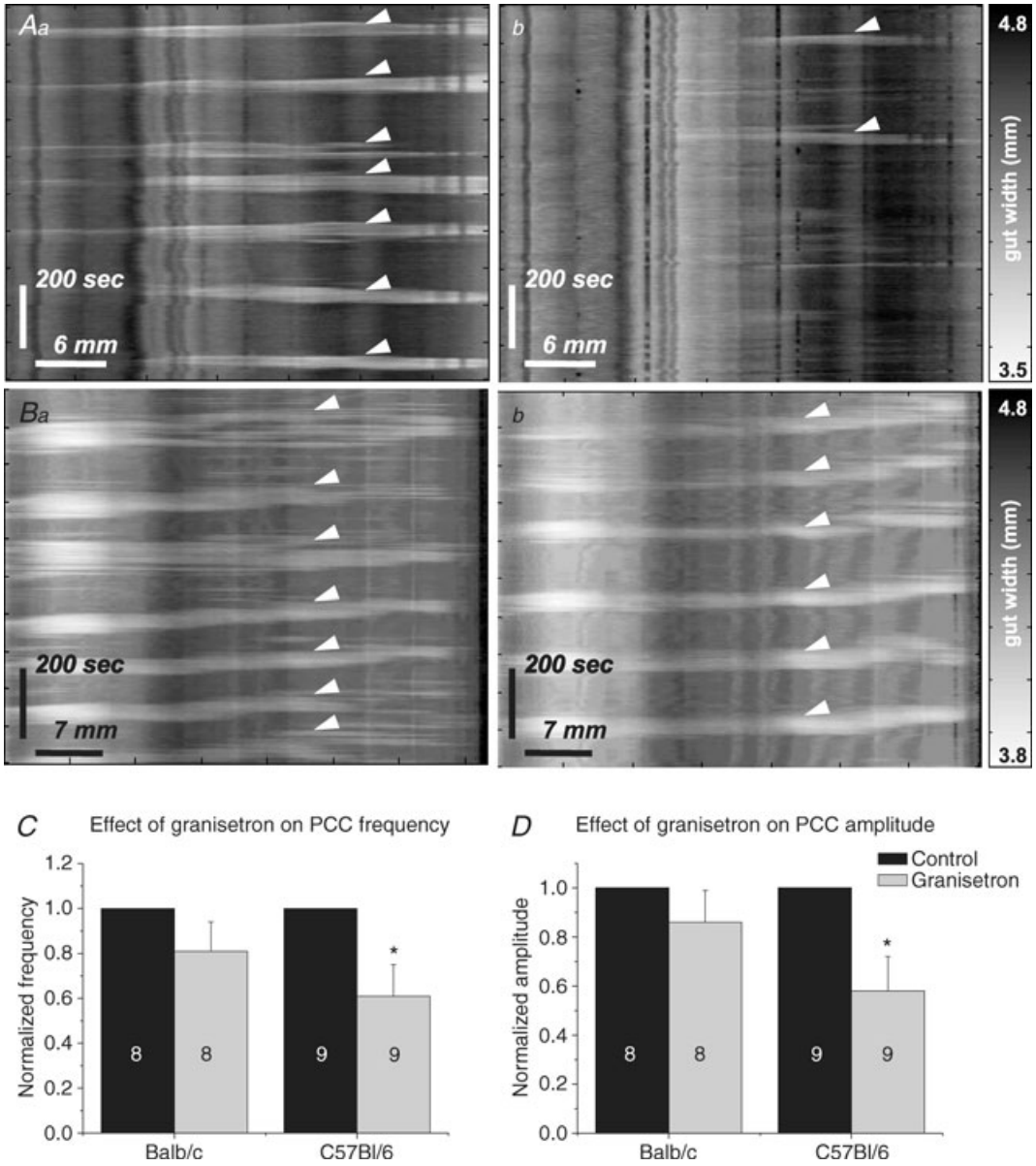

Figure 8. Effects of granisetron
Control PCCs (arrowheads) were observed in both C57Bl/6 (*Aa*) and Balb/c (*Ba*) mice. In granisetron, PCCs were significantly reduced in C57Bl/6 mice (*Ab*) but not in Balb/c mice (*Bb*). Granisetron-evoked reductions in frequency (*C*) and amplitude (*D*) tended to be observed in both strains when data were normalized to control. However, these reductions were only significant in C57Bl/6 mice (*$P < 0.05$).

C57Bl/6 from $72.9 \pm 8.6\%$ to $37.1 \pm 3.9\%$ maximum contraction; *t* test, $P < 0.01$), but the response remained comparable between strains. When granisetron (Fig. 10*C*) or combined granisetron and SB207266 (Fig. 10*D*) were added in the presence of methiothepin and ketanserin, further significant reduction in the response to exogenous 5-HT was observed in both Balb/c and C57Bl/6 mice (paired *t* test, $P < 0.01$). Strain had no affect on the response (ANOVA, $P < 0.01$).

Discussion

The present results demonstrate polymorphic *tph2* mRNA expression in LM-MP preparations from two inbred mouse strains. This finding strongly supports the suggestion that 5-HT-IR interneurones can synthesize 5-HT (Gershon, 2004) as well as transporting it from the extracellular space. The two strains also differ in the anatomy of serotonergic circuitry in the jejunal myenteric

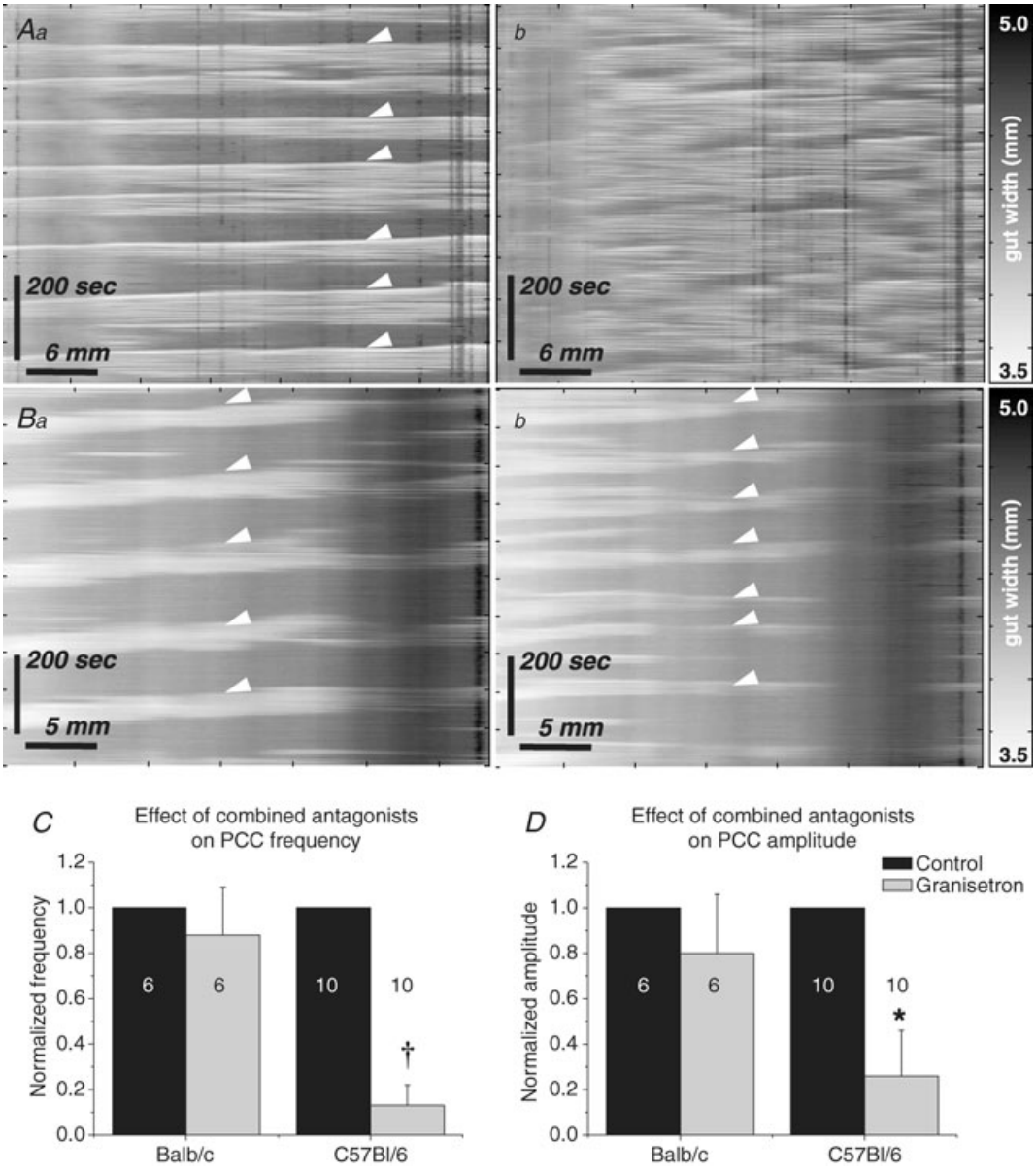

Figure 9. Effects of combined 5-HT antagonists
PCCs (arrowheads) were clearly observed in control conditions in C57Bl/6 (*Aa*) and Balb/c (*Ba*) mice. Application of combined antagonists frequently converted PCCs to irregular contractile activity (*Ab*) or abolished contractions completely in C57Bl/6 mice. In the majority of preparations in Balb/c mice, PCCs were not significantly affected by combined antagonists (*Bb*). Mean frequency (*C*; †$P < 0.01$) and amplitude (*D*; *$P < 0.05$) decreased significantly in C57Bl/6 mice only.

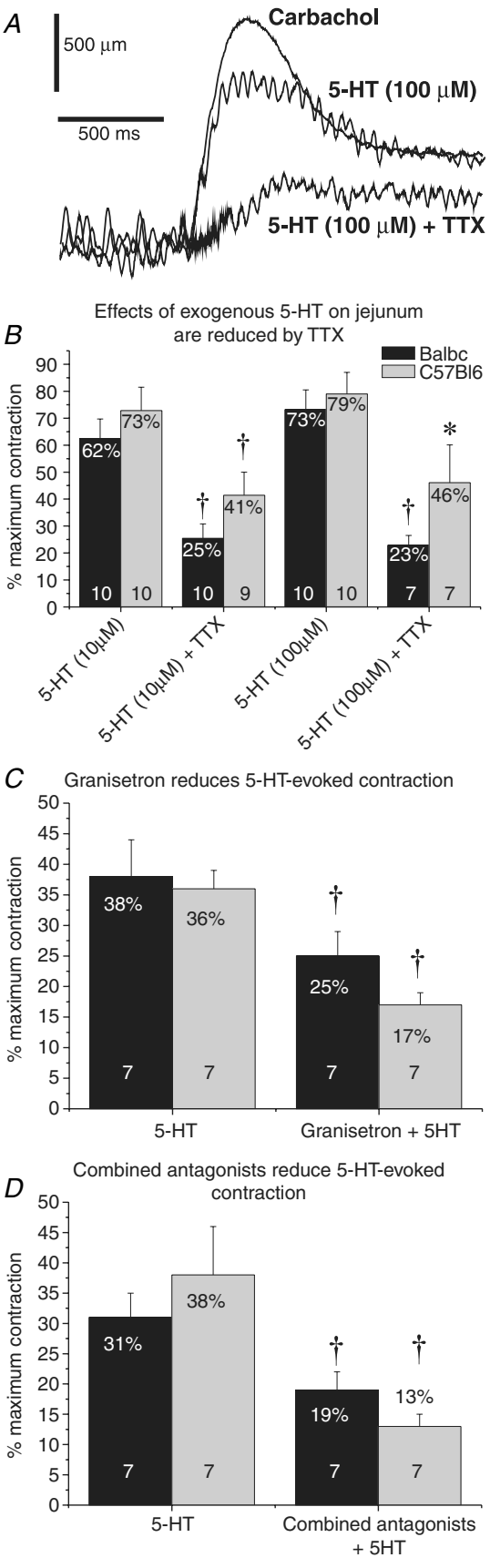

plexus. These differences in 5-HT-related genetics and anatomy between strains correlate with differences in sensitivity to 5-HT_3 and/or 5-HT_4 antagonists of a complex motility pattern (PCCs) in this intestinal region. Mice expressing a *tph2* genotype associated with low 5-HT synthesis (Balb/c; 1473G genotype) also had fewer anatomical connections to some neurochemically identified subtypes of neurones from 5-HT-IR interneurones, and were not sensitive to the antagonists in functional assays *in vitro* (Table 4). Mice expressing a *tph2* genotype associated with high 5-HT synthesis (C57Bl/6; 1473C genotype) had higher levels of 5-HT connectivity to some immunohistochemically defined neurones, and PCCs in these mice were sensitive to the antagonists (Table 4). Importantly, no parallel strain differences were detected in the pharmacology of jejunal responses to exogenous 5-HT. Thus, a murine *tph2* polymorphism known to affect available levels of endogenous 5-HT is associated with significant structural and functional consequences for enteric neural serotonergic pathways in the jejunum. The mechanisms by which these consequences occur remain to be elucidated. They presumably include developmental disturbances and differences in neurotransmission in mature reflex pathways, but are unlikely to include disruption of 5-HT receptor expression or activity in the adult.

tph2 expression and 5-HT synthesis

Expression of *tph2* mRNA was demonstrated in LM-MP preparations from three intestinal regions in this study. Transcripts were identified in samples of duodenum (Balb/c only), jejunum and colon (both strains) from adult mice. This indicates that *tph2* mRNA was expressed by neurones in these samples, since mucosa was not present, and mast cells express *tph1* (Sakowski *et al.* 2006*b*). These data localize *tph2* mRNA expression firmly within neurone-containing layers of the intestine. A previous study that reported *tph2* mRNA expression in duodenum appears to have used full-thickness samples of gut, incorporating mucosa (Côté *et al.* 2003), and

Figure 10. Intrinsic sensitivity of murine jejunum to 5-HT
Contractions were measured in longitudinally arranged segments of murine jejunum. *A*, example traces from a single segment in response to carbachol (maximal contraction), and to 5-HT (100 μM) alone and following incubation with TTX. All data were normalized to carbachol controls. *B*, 10 and 100 μM 5-HT evoked equally strong responses in both Balb/c and C57Bl/6 mice. TTX significantly reduced the 5-HT-evoked responses in both strains, but no strain differences in the residual responses were detected. In the presence of methiothepin (100 nM) and ketanserin (30 nm), granisetron alone (1 μm; *C*), and in combination with SB207266 (10 nm; *D*) significantly reduced responses to 10 μm 5-HT in both strains. No strain differences were detected in these responses. (*$P < 0.05$; †$P < 0.01$; * and † indicate comparisons within strains).

Table 4. Summary of genetic, anatomical and functional differences in neural 5-HT in jejunum of two inbred mouse strains

		Anatomy			Function (PCCs)		
Strain	Genotype	5-HT to NOS	5-HT to calretinin	5-HT to 5-HT	Granisetron	SB207266	Combined
Balb/c	1473G	Lower	Lower	Same	No effect	No effect	No effect
C57Bl/6	1473C	Higher	Higher	Same	↓ Frequency ↓ Amplitude	↓ Inhibition ratio	PCC abolished (80%)

therefore was not as definitive. The same study failed to show *tph2* expression in jejunum. The LM-MP samples used in the present study are rich in neurones, which constitute only a small proportion of cells in the whole gut. Thus, this discrepancy between previous reports and the present data probably arises from different sample selection. Previous studies have shown that LM-MP preparations can hydroxylate titrated L-tryptophan (Gershon *et al.* 1965; Lovenberg *et al.* 1967; Dreyfus *et al.* 1977*a*,*b*), and 5-HT can be detected in the duodenum of *tph1*$^{-/-}$ mice (Côté *et al.* 2003; Walther *et al.* 2003), implying TPH2 activity in this tissue. Furthermore, 5-HT-IR has been identified in neurones of *SERT*$^{-/-}$ mice (Chen *et al.* 2001). Thus, expression of *tph2* mRNA in LM-MP is consistent with earlier suggestions that some myenteric neurones synthesize 5-HT.

In the present study, Balb/c mice homozygously expressed mRNA for the 1473G allele, which is associated with significantly reduced synthetic capacity for 5-HT, and C57Bl/6 mice homozygously expressed the 1473C allele, which is associated with a higher synthetic capacity (Zhang *et al.* 2004; Cervo *et al.* 2005; Isles *et al.* 2005; Sakowski *et al.* 2006*a*). This single polymorphism in *tph2* accounts for the majority of inter-strain variance in 5-HT synthesis in the CNS among inbred mouse strains (Kulikov *et al.* 2007). These data therefore suggest that inbred mouse strains are likely to differ in levels of 5-HT synthesis by myenteric neurones.

Anatomy of 5-HT circuits in jejunal myenteric plexus

Counting varicosities that appear to be apposed to neurones at the limits of confocal microscope resolution is a method validated by electron microscopy for estimating synaptic connections between neurones (Mann *et al.* 1997). Confocal microscopy revealed strain differences in the numbers of connections identified in this manner between 5-HT interneurones and two neurochemically defined cell types in myenteric plexus of murine jejunum (Table 4). In C57Bl/6 mice, neurones immunoreactive for NOS and calretinin (non-Dogiel type II) were apposed by significantly larger numbers of 5-HT-IR varicosities than equivalent neurones in Balb/c mice, although the numbers of contacts were small in both strains. Interestingly, there was no corresponding difference in the numbers of 5-HT-IR varicosities apposed to 5-HT-IR neurones.

Comparatively little is known about the structure of the ENS in mouse, and few studies have attempted to correlate neurochemistry with morphology or function in this species and none in the jejunum (Furness *et al.* 2004; Nurgali *et al.* 2004; Mao *et al.* 2006). Certain neurochemical markers in mouse appear to have distributions similar to the better-described guinea pig ENS; for example, NOS labels inhibitory motor neurones and a population of interneurones with anally projecting axons, and 5-HT is confined to anally directed interneurones (Sang & Young, 1996; Sang *et al.* 1997; Brookes, 2001). However, other markers show a different distribution; for example, calretinin labels multi-axonal, AH/Dogiel type II sensory neurones in addition to excitatory motor neurones innervating both muscle coats, and a population of locally projecting interneurones (Sang & Young, 1996, 1998; Sang *et al.* 1997; Furness *et al.* 2004; Nurgali *et al.* 2004). Although the absolute numbers of connections observed in the current study were small, presumed 5-HT contacts on both NOS- and calretinin-IR neurones were significantly more numerous in C57Bl/6 mice than in Balb/c. In murine sympathetic ganglia, electron and confocal microscopic analyses have shown that synapses are randomly distributed across the surface of neurones, and that the total number of synapses is proportional to the surface area of a neurone (Gibbins *et al.* 1998, 2000). The sizes of NOS-IR neurones in guinea pig jejunum have been estimated, and range from 360 to 2100 μm^2, with a mean of 858 μm^2 ($n = 58$, data from Neal & Bornstein, 2007*a*). This is substantially larger than the mean sizes estimated for NOS-IR neurones in the jejunum of either strain in the present study. It is likely that the small numbers of connections observed in murine jejunum were proportional to neurone size. Thus, 5-HT interneurones may play a greater role in motility reflexes involving both inhibitory and excitatory motor neurones, and/or in the propagation of reflexes between locally and anally projecting interneurones in C57Bl/6 mice than in Balb/c mice.

5-HT is a developmental signal in the early postnatal mouse ENS (Fiorica-Howells *et al.* 2000), and the *mash1*-dependent 5-HT neurones differentiate (Pham *et al.* 1991; Blaugrund *et al.* 1996) and acquire their

neurotransmitter (Rothman & Gershon, 1982) early. At this developmental stage, 5-HT acts via 5-HT_{2B} receptors to stimulate neurite branching in a subset of enteric neurones (Fiorica-Howells *et al.* 2000). However, the mechanisms controlling synaptogenesis in the developing ENS have not been examined. It is possible that the low synthetic capacity of TPH2, and consequent low myenteric 5-HT levels in Balb/c mice during ENS development, lead to decreased axonal branching in 5-HT neurones and, thus, to the reduced connectivity observed in adult animals in this study. This hypothesis remains to be tested directly.

Strain-specific effects of 5-HT_3 and 5-HT_4 antagonists on a complex jejunal motility pattern

In the present study, 5-HT_3 and 5-HT_4 antagonists varied in their ability to inhibit jejunal PCCs depending on strain (Table 4); C57Bl/6 jejunum showed a consistently greater sensitivity to 5-HT_3 and 5-HT_4 antagonism than Balb/c jejunum. These data in C57Bl/6 jejunum are in broad agreement with the existing literature concerning 5-HT_3 and 5-HT_4 receptor-mediated effects on PCC-like activity and transit in the small intestine (Brown *et al.* 1993; Nagakura *et al.* 1996; Yamamoto *et al.* 1999; Bush *et al.* 2001). The insensitivity of Balb/c jejunum to the antagonists correlated with the reduced anatomical connectivity of jejunal 5-HT neurones in this strain. The observed strain difference in function might arise from compensatory remodelling leading to other neurones undertaking some normal functions of 5-HT interneurones, or to an altered contribution of co-transmitters associated with low 5-HT synthesis.

The strength of anatomical 5-HT connections to neurones in motility reflex pathways could influence the importance of 5-HT neurotransmission in those reflexes. The lower connectivity between 5-HT interneurones and excitatory motor neurones (calretinin-IR), inhibitory motor neurones (NOS-IR) and/or NOS descending interneurones in Balb/c mice may indicate that 5-HT plays a reduced role in direct excitation of neurones in excitatory and inhibitory motor pathways in this strain. This would be expected to lead to a reduced sensitivity of motor patterns mediated by these pathways to the antagonists. The insensitivity of jejunal PCCs to 5-HT_3 and 5-HT_4 receptor antagonism might also arise from adaptations in the 5-HT signalling system in response to low transmitter levels. For example, inflammation enhances the contribution of 5-HT_3 receptors to fast EPSPs in submucous neurones by increasing the ratio of 5-HT to ACh released by presynaptic terminals (Lomax *et al.* 2005). It is possible that levels of available 5-HT similarly influence relative synaptic contribution. In addition, genetic differences in other elements of the 5-HT or other relevant signalling pathways may also segregate between strains, contributing to the functional and anatomical outcomes observed in the current study. A role for hitherto-unidentified strain differences in *tph1*, *SERT* or genes encoding other relevant proteins cannot be excluded.

Responses to exogenous 5-HT are unaffected by *tph2* polymorphism

Although sensitivity of PCCs to granisetron and combined antagonists differed between strains, the present data provide evidence that jejunal tissues in Balb/c and C57Bl/6 mice are equally sensitive to exogenously applied 5-HT. Exogenous 5-HT excited receptors on muscle and neurones in both strains; these responses were similar between strains, and were reduced to similar degrees by a range of 5-HT receptor antagonists in both Balb/c and C57Bl/6 mice. Thus, the different sensitivities to 5-HT receptor antagonism observed in *in vitro* behavioural assays were unlikely to arise from differences in receptor expression or activity. Rather, it is more likely that they arise from compensatory neurotransmission by alternate neurotransmitters and/or types of neurone regulating this behaviour in mice where endogenous 5-HT is low. The identity of such potential alternate transmitters or neurones remains unknown.

Conclusions

This study demonstrates a correlation between genetic, anatomical and functional disturbances in neural 5-HT in the jejunum of two inbred mouse strains. These data suggest that different synthetic capacity for 5-HT in enteric neurones, conferred by polymorphisms in *tph2,* is associated with modified development and mature function of enteric serotonergic circuits. The precise mechanisms by which these three levels of strain differences are linked remain to be elucidated, but may include altered neurite development of perinatal enteric neurones, and/or altered neurotransmission in response to 5-HT levels in the adult, in the absence of differences in intrinsic sensitivity to 5-HT. These associative findings require further investigation. Functional polymorphisms in *tph2* have been demonstrated in humans (Zhang *et al.* 2005, 2006). Thus, the present data suggest that *tph2* genotype may underlie refraction to 5-HT-directed therapies in human patients suffering bowel disorders. These data also demonstrate the importance of strain selection when investigating the role of enteric neural 5-HT in mice.

References

Abdu F, Hicks GA, Hennig G, Allen JP & Grundy D (2002). Somatostatin Sst_2 receptors inhibit peristalsis in the rat and mouse jejunum. *Am J Physiol Gastrointest Liver Physiol* **282**, G624–G633.

Anlauf M, Schafer MKH, Eiden L & Weihe E (2003). Chemical coding of the human gastrointestinal nervous system: cholinergic, VIPergic, and catecholaminergic phenotypes. *J Comp Neurol* **459**, 90–111.

Barbiers M, Timmermans JP, Adriaensen D, Degroodtlasseel MHA & Scheuermann DW (1995). Projections of neurochemically specified neurons in the porcine colon. *Histochem Cell Biol* **103**, 115–126.

Bertrand PP (2006). Real-time measurement of serotonin release and motility in guinea pig ileum. *J Physiol* **577**, 689–704.

Blaugrund E, Pham TD, Tennyson VM, Lo L, Sommer L, Anderson DJ & Gershon MD (1996). Distinct subpopulations of enteric neuronal progenitors defined by time of development, sympathoadrenal lineage markers and Mash-1-dependence. *Development* **122**, 309–320.

Brookes SJH (2001). Classes of enteric nerve cells in the guinea-pig small intestine. *Anat Rec* **262**, 58–70.

Brown NJ, Horton A, Rumsey RDE & Read NW (1993). Granisetron and ondansetron – effects on the ileal brake mechanism in the rat. *J Pharm Pharmacol* **45**, 521–524.

Bush TG, Spencer NJ, Watters N, Sanders KM & Smith TK (2001). Effects of alosetron on spontaneous migrating motor complexes in murine small and large bowel *in vitro*. *Am J Physiol Gastrointest Liver Physiol* **281**, G974–G983.

Calcagno E, Canetta A, Guzzetti S, Cervo L & Invernizzi RW (2007). Strain differences in basal and post-citalopram extracellular 5-HT in the mouse medial prefrontal cortex and dorsal hippocampus: relation with tryptophan hydroxylase-2 activity. *J Neurochem* **103**, 1111–1120.

Cervo L, Canetta A, Calcagno E, Burbassi S, Sacchetti G, Caccia S, Fracasso C, Albani D, Forloni G & Invernizzi RW (2005). Genotype-dependent activity of tryptophan hydroxylase-2 determines the response to citalopram in a mouse model of depression. *J Neurosci* **25**, 8165–8172.

Chen JJ, Li ZS, Pan H, Murphy DL, Tamir H, Koepsell H & Gershon MD (2001). Maintenance of serotonin in the intestinal mucosa and ganglia of mice that lack the high-affinity serotonin transporter: abnormal intestinal motility and the expression of cation transporters. *J Neurosci* **21**, 6348–6361.

Chen JJ, Wan S & Gershon MD (2004). Expression of two isoforms of tryptophan hydroxylase (Tph-1 and Tph-2) in the human and mouse gut. *Gastroenterology* **126**, A411.

Costa M, Furness JB, Cuellot AC, Verhofstad AAJ, Steinbusch HWJ & Elde RP (1982). Neurons with 5-hydroxytryptamine-like immunoreactivity in the enteric nervous system: their visualization and reactions to drug treatment. *Neuroscience* **7**, 351–363.

Côté F, Thévenot E, Fligny C, Fromes Y, Darmon M, Ripoche M-A, Bayard E, Hanoun N, Saurini F, Lechat P, Dandolo L, Hamon M, Mallet J & Vodjdani G (2003). Disruption of the nonneural *tph1* gene demonstrates the importance of peripheral serotonin in cardiac function. *Proc Nat Acad Sci U S A* **100**, 13525–13530.

Crowley JJ, Blendy JA & Lucki I (2005). Strain-dependent antidepressant-like effects of citalopram in the mouse tail suspension test. *Psychopharmacology* **183**, 257–264.

Dreyfus CF, Bornstein MB & Gershon MD (1977*a*). Synthesis of serotonin by neurons of the myenteric plexus in situ and in organotypic tissue culture. *Brain Res* **128**, 125–139.

Dreyfus CF, Sherman DL & Gershon MD (1977*b*). Uptake of serotonin by intrinsic neurons of the myenteric plexus grown in organotypic tissue culture. *Brain Res* **128**, 109–123.

Englander MT, Dulawa SC, Bhansali P & Schmauss C (2005). How stress and fluoxetine modulate serotonin 2C receptor pre-mRNA editing. *J Neurosci* **25**, 648–651.

Fida R, Bywater RAR, Lyster DJK & Taylor GS (2000). Chronotropic action of 5-hydroxytryptamine (5-HT) on colonic migrating motor complexes (CMMCs) in the isolated mouse colon. *J Auton Nerv Syst* **80**, 52–63.

Fiorica-Howells E, Maroteaux L & Gershon MD (2000). Serotonin and the 5-HT_{2B} receptor in the development of enteric neurons. *J Neurosci* **20**, 294–305.

Furness JB, Robbins HL, Xiao JH, Stebbing MJ & Nurgali K (2004). Projections and chemistry of Dogiel type II neurons in the mouse colon. *Cell Tissue Res* **317**, 1–12.

Galligan JJ & Parkman HP (2007). Recent advances in understanding the role of serotonin in gastrointestinal motility and functional bowel disorders. *Neurogastroenterol Motil* **19**, 1–4.

Gershon MD (2004). Serotonin receptors and transporters – roles in normal and abnormal gastrointestinal motility (Review article). *Aliment Pharmacol Ther* **20**, 3–14.

Gershon MD, Drakontides AB & Ross LL (1965). Serotonin: synthesis and release from the myenteric plexus of the mouse intestine. *Science* **149**, 197–199.

Gershon MD & Tack J (2007). The serotonin signaling system: from basic understanding to drug development-for functional GI disorders. *Gastroenterology* **132**, 397–414.

Gibbins IL, Jobling P, Messenger JP, Teo EH & Morris JL (2000). Neuronal morphology and the synaptic organisation of sympathetic ganglia. *J Auton Nerv Syst* **81**, 104–109.

Gibbins IL, Rodgers HF, Matthew SE & Murphy SM (1998). Synaptic organisation of lumbar sympathetic ganglia of guinea pigs: serial section ultrastructural analysis of dye-filled sympathetic final motor neurons. *J Comp Neurol* **402**, 285–302.

Grider JR, Foxx-Orenstein AE & Jin J-G (1998). 5-Hydroxytryptamine4 receptor agonists initiate the peristaltic reflex in human, rat, and guinea pig intestine. *Gastroenterology* **115**, 370–380.

Grider JR, Kuemmerle JF & Jin J-G (1996). 5-HT released by mucosal stimuli initiates peristalsis by activating 5-HT_4/5-HT_{1P} receptors on sensory Cgrp neurons. *Am J Physiol Gastrointest Liver Physiol* **270**, G778–G782.

Gwynne RM, Thomas EA, Goh SM, Sjövall H & Bornstein JC (2004). Segmentation induced by intraluminal fatty acid in isolated guinea-pig duodenum and jejunum. *J Physiol* **556**, 557–569.

Hackler EA, Airey DC, Shannon CC, Sodhi MS & Sanders-Bush E (2006). 5-HT_{2C} receptor RNA editing in the amygdala of C57Bl/6J, DBA/2J, and Balb/cJ mice. *Neurosci Res* **55**, 96–104.

Haycock JW & Waymire JC (1982). Activating antibodies to tyrosine-hydroxylase. *J Biol Chem* **257**, 9416–9423.

Isles AR, Hathway GJ, Humby T, de la Riva C, Kendrick KM & Wilkinson LS (2005). An Mtph2 SNP gives rise to alterations in extracellular 5-HT levels, but not in performance on a delayed-reinforcement task. *Eur J Neurosci* **22**, 997–1000.

Izikki M, Hanoun N, Marcos E, Savale L, Barlier-Mur AM, Saurini F, Eddahibi S, Hamon M & Adnot S (2007). Tryptophan hydroxylase 1 knockout and tryptophan hydroxylase 2 polymorphism: effects on hypoxic pulmonary hypertension in mice. *Am J Physiol Lung Cell Mol Physiol* **293**, L1045–L1052.

Kadowaki M, Wade PR & Gershon MD (1996). Participation of 5-HT_3, 5-HT_4, and nicotinic receptors in the peristaltic reflex of guinea pig distal colon. *Am J Physiol Gastrointest Liver Physiol* **271**, G849–G857.

Kulikov AV, Osipova DV, Naumenko VS & Popova NK (2005). Association between Tph2 gene polymorphism, brain tryptophan hydroxylase activity and aggressiveness in mouse strains. *Genes, Brain Behav* **4**, 482–485.

Kulikov AV, Osipova DV & Popova NK (2007). The C1473G polymorphism in gene tph2 is the main factor mediating the genetically defined variability of tryptophan hydroxylase-2 activity in the mouse brain (in Russian). *Genetika* **43**, 1676–1681.

Lomax AE, Mawe GM & Sharkey KA (2005). Synaptic facilitation and enhanced neuronal excitability in the submucosal plexus during experimental colitis in guinea-pig. *J Physiol* **564**, 863–875.

Lovenberg W, Jequier E & Sjoerdsma A (1967). Tryptophan hydroxylation: measurement in pineal gland, brainstem, and carcinoid tumor. *Science* **155**, 217–219.

Mann PT, Southwell BR, Young HM & Furness JB (1997). Appositions made by axons of descending interneurons in the guinea-pig small intestine, investigated by confocal microscopy. *J Chem Neuroanat* **12**, 151–164.

Mao YK, Wang BX & Kunze W (2006). Characterization of myenteric sensory neurons in the mouse small intestine. *J Neurophysiol* **96**, 998–1010.

Nagakura Y, Kontoh A, Tokita K, Tomoi M, Shimomura K & Kadowaki M (1997). Combined blockade of 5-HT_3- and 5-HT_4-serotonin receptors inhibits colonic functions in conscious rats and mice. *J Pharmacol Exp Ther* **281**, 284–290.

Nagakura Y, Naitoh Y, Kamato T, Yamano M & Miyata K (1996). Compounds possessing 5-HT_3 receptor antagonistic activity inhibit intestinal propulsion in mice. *Eur J Pharmacol* **311**, 67–72.

Neal KB & Bornstein JC (2006). Serotonergic receptors in therapeutic approaches to gastrointestinal disorders. *Curr Opin Pharmacol* **6**, 547–552.

Neal KB & Bornstein JC (2007*a*). Mapping serotonin inputs to enteric neurons of the guinea pig small intestine. *Neuroscience* **145**, 556–567.

Neal KB & Bornstein JC (2007*b*). Strain differences in tph2 genotype in murine myenteric neurons. *Auton Neurosci* **135**, 98–99.

Neal KB & Bornstein JC (2008*a*). Enteric 5-HT circuits differ between inbred mouse strains. *Proc Aust Neurosci Soc* **18**, 43.

Neal KB & Bornstein JC (2008*b*). Targets of myenteric interneurons in the guinea-pig small intestine. *Neurogastroenterol Motil* **20**, 566–575.

Neal KB, Parry LJ & Bornstein JC (2008). Strain-specific expression of Tph2 polymorphism in murine enteric neurons. *Gastroenterology* **134**, A685.

Nurgali K, Stebbing MJ & Furness JB (2004). Correlation of electrophysiological and morphological characteristics of enteric neurons in the mouse colon. *J Comp Neurol* **468**, 112–124.

Pham TD, Gershon MD & Rothman TP (1991). Time of origins of neurons in the murine enteric nervous system – sequence in relation to phenotype. *J Comp Neurol* **314**, 789–798.

Popova NK (2006). From genes to aggressive behavior: the role of serotonergic system. *Bioessays* **28**, 495–503.

Roberts RR, Bornstein JC, Bergner AJ & Young HM (2008). Disturbances of colonic motility in mouse models of Hirschsprung's disease. *Am J Physiol Gastroint Liver Physiol* **294**, G996–G1008.

Roberts RR, Murphy JF, Young HM & Bornstein JC (2007). Development of colonic motility in the neonatal mouse – studies using spatiotemporal maps. *Am J Physiol Gastroint Liver Physiol* **292**, G930–G938.

Rothman TP & Gershon MD (1982). Phenotypic-expression in the developing murine enteric nervous-system. *J Neurosci* **2**, 381–393.

Sakowski SA, Geddes TJ & Kuhn DM (2006*a*). Mouse tryptophan hydroxylase isoform 2 and the role of proline 447 in enzyme function. *J Neurochem* **96**, 758–765.

Sakowski SA, Geddes TJ, Thomas DM, Levi E, Hatfield JS & Kuhn DM (2006*b*). Differential tissue distribution of tryptophan hydroxylase isoforms 1 and 2 as revealed with monospecific antibodies. *Brain Res* **1085**, 11–18.

Sang Q, Williamson S & Young HM (1997). Projections of chemically identified myenteric neurons of the small and large intestine of the mouse. *J Anat* **190**, 209–222.

Sang Q & Young HM (1996). Chemical coding of neurons in the myenteric plexus and external muscle of the small and large intestine of the mouse. *Cell Tissue Res* **284**, 39–53.

Sang Q & Young HM (1998). The identification and chemical coding of cholinergic neurons in the small and large intestine of the mouse. *Anat Rec* **251**, 185–199.

Seerden TC, Lammers WJ, De Winter BY, De Man JG & Pelckmans PA (2005). Spatiotemporal electrical and motility mapping of distension-induced propagating oscillations in the murine small intestine. *Am J Physiol Gastrointest Liver Physiol* **289**, G1043–G1051.

Sharkey KA, Lomax AEG, Bertrand PP & Furness JB (1998). Electrophysiology, shape, and chemistry of neurons that project from guinea pig colon to inferior mesenteric ganglia. *Gastroenterology* **115**, 909–918.

Tonini M (2005). 5-Hydroxytryptamine Effects in the Gut: The 3, 4, and 7 Receptors. *Neurogastroenterol Motil* **17**, 637–642.

Walther DJ & Bader M (2003). A unique central tryptophan hydroxylase isoform. *Biochem Pharmacol* **66**, 1673–1680.

Walther DJ, Peter J-U, Bashammakh S, Hörtnagl H, Voits M, Fink H & Bader M (2003). Synthesis of serotonin by a second tryptophan hydroxylase isoform. *Science* **299**, 76.

Wardell CF, Bornstein JC & Furness JB (1994). Projections of 5-hydroxytryptamine-immunoreactive neurons in guinea-pig distal colon. *Cell Tissue Res* **278**, 379–387.

Williamson S, Pompolo S & Furness JB (1996). GABA and nitric oxide synthase immunoreactivities are colocalized in a subset of inhibitory motor neurons of the guinea-pig small intestine. *Cell Tissue Res* **284**, 29–37.

Yamamoto I, Kuwahara A, Fujimura M, Kadowaki M & Fujiyama M (1999). Involvement of 5-HT_3 and 5-HT_4 receptors in the motor activity of isolated vascularly perfused rat duodenum. *Neurogastroenterol Motil* **11**, 457–465.

Young HM & Furness JB (1995). Ultra-structural examination of the targets of serotonin-immunoreactive descending interneurons in the guinea-pig small intestine. *J Comp Neurol* **356**, 101–114.

Zhang X, Beaulieu JM, Gainetdinov R & Caron MG (2006). Functional polymorphisms of the brain serotonin synthesizing enzyme tryptophan hydroxylase-2. *Cell Mol Life Sci* **63**, 6–11.

Zhang XD, Beaulieu JM, Sotnikova TD, Gainetdinov RR & Caron MG (2004). Tryptophan hydroxylase-2 controls brain serotonin synthesis. *Science* **305**, 217–217.

Zhang XD, Gainetdinov RR, Beaulieu JM, Sotnikova TD, Burch LH, Williams RB, Schwartz DA, Krishnan KRR & Caron MG (2005). Loss-of-function mutation in tryptophan hydroxylase-2 identified in unipolar major depression. *Neuron* **45**, 11–16.

Acknowledgements

The authors wish to acknowledge Ms Melina Ellis, Ms Kirsty Turner and Ms Rachel Gwynne for their technical assistance, and Associate Professor Heather Young for comments on the manuscript. Funding for this work was provided by the National Health & Medical Research Council of Australia (Dora Lush Postgraduate Research Scholarship no. 400484 (K.B.N.) and Project Grant no. 400053 (J.C.B.)).